

Aberrant Plasma Cells in the Absence of M-Protein: Ancillary Testing beyond Protein Electrophoresis

Lechuang Chen,^a Nourhan Garnal Elgela Ibrahim,^b Guilin Tang,^c Qing H. Meng,^a and Zhihong Hu^{a,*}

^aDepartment of Laboratory Medicine, The University of Texas MD Anderson Cancer Center, Houston, TX, United States;

^bDepartment of Pathology and Laboratory Medicine, The University of Texas Health Science Center, Houston, TX, United States;

^cDepartment of Hematopathology, The University of Texas MD Anderson Cancer Center, Houston, TX, United States.

*Address correspondence to this author at: Department of Laboratory Medicine, The University of Texas MD Anderson Cancer Center, 1515 Holcombe Blvd, Houston, TX 77030-4009, United States. E-mail ZHu6@mdanderson.org.

CASE DESCRIPTION

A 65-year-old female initially presented in October 2020 with multilevel vertebral compression fractures. Histological evaluation of biopsy specimens from the L1 and L3 vertebrae demonstrated sheets of neoplastic plasma cells. Immunohistochemical studies showed that the neoplastic cells were positive for BCL2, CD138, cyclin D1, and MUM1/IRF4, with variable expression of CD20. They were negative for CD3, CD5, CD10, CD23, and BCL6 stains. A subsequent bone marrow biopsy in early November 2020 revealed >95% involvement by plasma cells forming sheets. Flow cytometry revealed a population of plasma cells lacking CD56 and showing absence of both surface and cytoplasmic light-chain expression. Fluorescence in situ hybridization (FISH) confirmed the presence of *t*(11;14) and monosomy 13. Based on all these findings, a diagnosis of plasma cell myeloma was established.

The patient subsequently initiated treatment with a daratumumab, lenalidomide, and dexamethasone regimen, and was admitted to our institution for further therapy in February 2021. Serum and urine protein electrophoresis and immunofixation were performed on March 1, 2021. Serum protein electrophoresis (SPEP) revealed a small peak at the junction between the mid-gamma and slow-gamma regions. Hypogammaglobulinemia was also noted. Serum immunofixation (SIFE) using antisera against IgG, IgA, IgM, and bound/free kappa light chains showed no definitive evidence of an M-protein band. However, a small IgG kappa band was present in the gamma region. Given the patient's treatment with daratumumab, this small band represented the presence of therapeutic monoclonal antibody (Fig. 1A). This interpretation was supported by the band's mobility, timing with drug administration, and lack of clonal plasma cell markers. Serum free light chain (FLC) levels below detection limits (free kappa <1.18 mg/dL, RI: 3.30–19.40 mg/dL; free lambda <1.47 mg/dL, RI: 5.71–26.30 mg/dL). The urine protein electrophoretic pattern did not show definite evidence of a Bence–Jones protein peak. The urine protein immunofixation electrophoretic patterns obtained with the use of antisera against IgG, IgA, IgM, bound kappa and bound lambda light chains, and free kappa and free lambda light-chain proteins did not show definite evidence of a Bence–Jones proteinuria (Fig. 1B).

The patient underwent a bone marrow biopsy at our institution on March 15, 2021. Bone marrow biopsy continued to show sheets of atypical plasma cells comprising approximately 80% of the medullary space. Many were atypical, of intermediate size with open chromatin and lacking perinuclear hof formation. Flow-cytometric immunophenotyping, performed on the aspirate, identified an aberrant plasma cell population with no kappa or lambda light-chain expression (Fig. 1C). After completing 4 cycles of daratumumab-based therapy, she underwent autologous stem cell transplantation (ASCT) in October 2021. Despite treatment, the patient continued to experience persistent and severe pain, predominantly attributed to postherpetic neuralgia and residual vertebral damage. Additional complications included anemia and Wernicke encephalopathy. She remained on maintenance therapy following ASCT. A peripheral-blood smear review in January 2024 demonstrated pancytopenia with approximately 23% circulating plasma cells. These plasma cells were characterized by eccentric nuclei, basophilic cytoplasm,

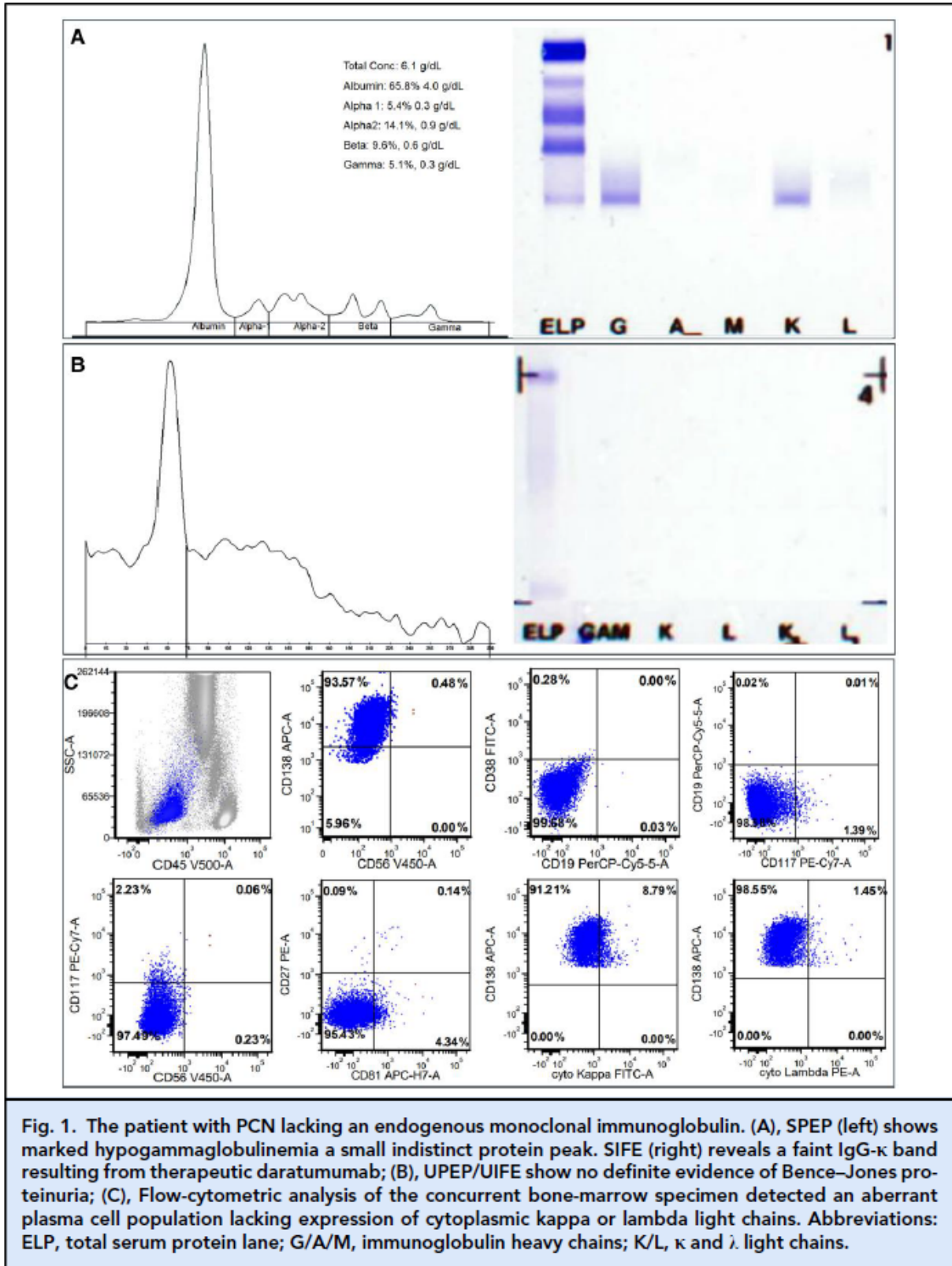
and inconspicuous nucleoli (Fig. 2A). SPEP, SIFE, and urine studies continued to show no detectable M-protein (Fig. 2B). Bone-marrow biopsy confirmed plasma cell leukemia (PCL), involving >95% of marrow cellularity, as highlighted by CD138 immunostaining on both biopsy and clot sections (Fig. 2C). Next-generation sequencing (NGS) identified multiple mutations involving *TP53* [c.634T>A (p.F212I), variant allele frequency (VAF) 49%], *CCND1* [c.130T>G (p.Y44D) VAF 47%, c.149A>G (p.K50R) VAF 46%], *KMT2D* [c.8488C>T (p.R2830*), VAF 29%], *PTPN11* [c.182A>T (p.D61V) VAF 31%], and *BCL6* [c.1370C>T (p.S457F) VAF 47%], consistent with high-risk disease. Optical genome mapping (OGM) and FISH revealed complex genomic rearrangements including *t*(11;14), *t*(14;20), and *MYC* rearrangements, and monosomy 13, indicating significant genomic instability associated with aggressive disease progression (Fig. 2D).

Further laboratory studies revealed profound hypogammaglobulinemia with hypoalbuminemia (3.2 g/dL, RI: 3.5–5.2 g/dL) and markedly reduced immunoglobulin levels (IgG 296 mg/dL, RI: 610.0–1616.0 mg/dL; IgM 12 mg/dL, RI: 35.0–242.0 mg/dL; IgA 37 mg/dL, RI: 85.0–499.0 mg/dL), and elevated beta-2 microglobulin and lactate dehydrogenase levels. Imaging studies demonstrated aggressive disease progression. Fluorodeoxyglucose positron emission tomography revealed increased fluorodeoxyglucose avidity throughout skeletal structures. Repeat bone-marrow biopsy confirmed nearly complete infiltration by malignant plasma cells, corroborating extensive disease involvement.

The patient was admitted again to the emergency room in June 2024 due to hypercalcemia (calcium 11.1 mg/dL, RI: 8.2–10.2 mg/dL), elevated lactate dehydrogenase (1920 U/L, RI: 135–214 U/L), and liver dysfunction indicated by significantly increased alkaline phosphatase (411 U/L, RI: 35–104 U/L), increased alanine aminotransferase (165 U/L, RI: ≤ 33 U/L), elevated bilirubin (total bilirubin 2.8 mg/dL, RI: 0.0–1.2 mg/dL; and direct bilirubin 1.4 mg/dL, RI: 0.0–0.3 mg/dL). Despite aggressive management including intravenous hydration, bisphosphonates (zoledronic acid), calcitonin therapy, and supportive care, the patient's disease progressed. Then the patient transitioned to hospice care, where she ultimately succumbed to progressive disease on June 22, 2024.

QUESTIONS TO CONSIDER	
1.	What are the key diagnostic challenges in nonsecretory PCL compared to secretory PCL?
2.	How does the absence of surface and cytoplasmic light-chain expression on flow cytometry affect the diagnosis and monitoring of nonsecretory PCL?
3.	How can molecular testing help overcome the limitations posed by the absence of detectable M-protein in nonsecretory PCL?
4.	What is the clinical significance of detecting <i>MYC</i> rearrangement in plasma cell neoplasms?
5.	What are the recommended treatment regimens for patients with nonsecretory PCL?

Continued on the next page....



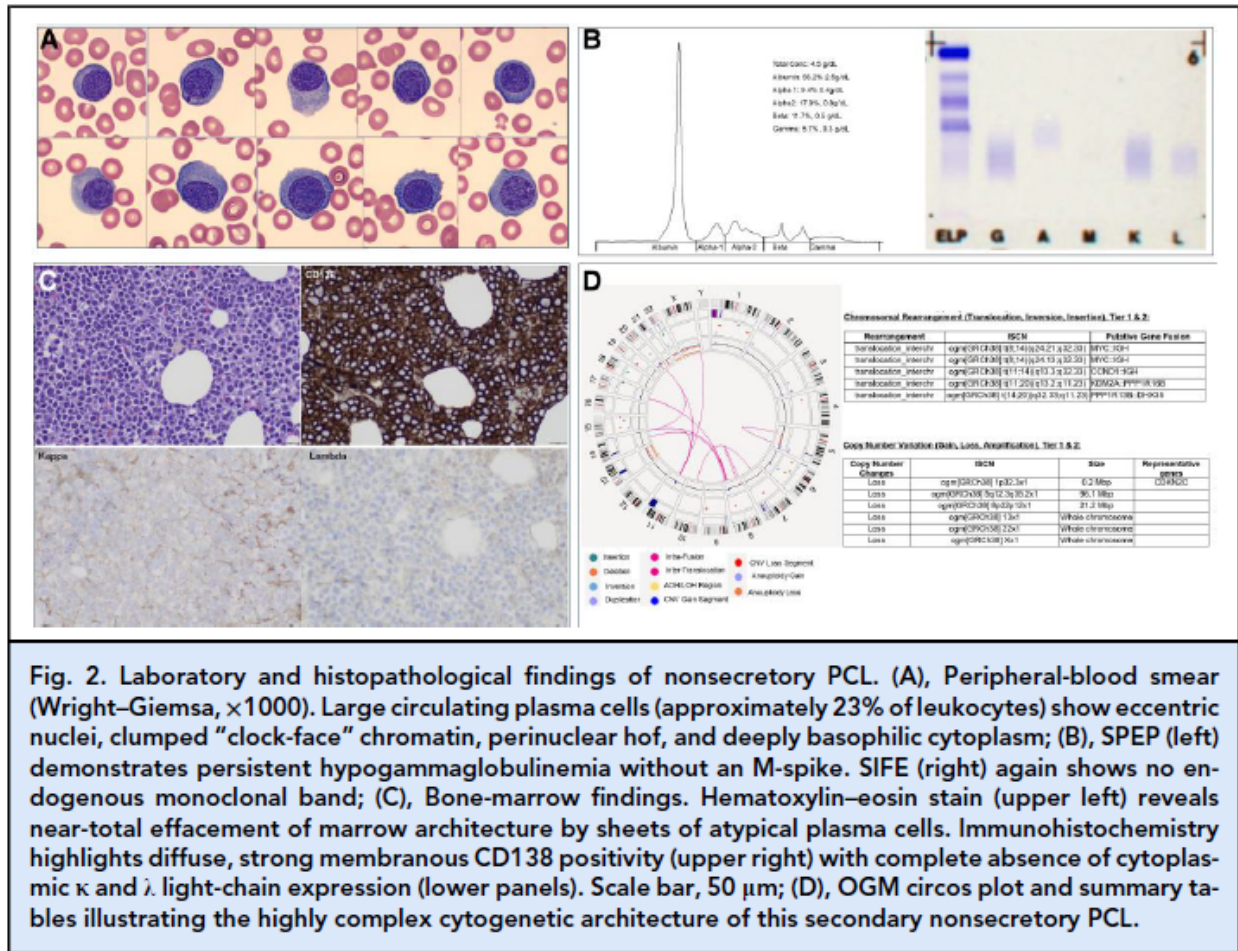


Fig. 2. Laboratory and histopathological findings of nonsecretory PCL. (A), Peripheral-blood smear (Wright–Giemsa, ×1000). Large circulating plasma cells (approximately 23% of leukocytes) show eccentric nuclei, clumped “clock-face” chromatin, perinuclear hof, and deeply basophilic cytoplasm; (B), SPEP (left) demonstrates persistent hypogammaglobulinemia without an M-spike. SIFE (right) again shows no endogenous monoclonal band; (C), Bone-marrow findings. Hematoxylin–eosin stain (upper left) reveals near-total effacement of marrow architecture by sheets of atypical plasma cells. Immunohistochemistry highlights diffuse, strong membranous CD138 positivity (upper right) with complete absence of cytoplasmic κ and λ light-chain expression (lower panels). Scale bar, 50 μm; (D), OGM circos plot and summary tables illustrating the highly complex cytogenetic architecture of this secondary nonsecretory PCL.

Final Publication and Comments

The final published version with discussion and comments from the experts will appear in the December 2025 issue of *Clinical Chemistry*. To view the case and comments online, go to <https://academic.oup.com/clinchem/issue/71/12> and follow the link to the Clinical Case Study and Commentaries.

Educational Centers

If you are associated with an educational center and would like to receive the cases and questions 1 month in advance of publication, please email clinchemed@myadlm.org.

All previous Clinical Case Studies can be accessed and downloaded online at <https://www.myadlm.org/science-and-research/clinical-chemistry/clinical-case-studies>.

ADLM (formerly AACC) is pleased to allow free reproduction and distribution of this Clinical Case Study for personal or classroom discussion use. When photocopying, please make sure the DOI and copyright notice appear on each copy.

ADLM (formerly AACC) is a leading professional society dedicated to improving healthcare through laboratory medicine. Its nearly 10,000 members are clinical laboratory professionals, physicians, research scientists, and others involved in developing tests and directing laboratory operations. ADLM brings this community together with programs that advance knowledge, expertise, and innovation. ADLM is best known for the respected scientific journal *Clinical Chemistry* and the world's largest conference on laboratory medicine and technology. Through these and other programs, ADLM advances laboratory medicine and the quality of patient care.